Article

Kinetics and Mechanism of Olefin Epoxidation with Aqueous HO and a Highly Selective Surface-Modified TaSBA15 Heterogeneous Catalyst

Daniel A. Ruddy, and T. Don Tilley

J. Am. Chem. Soc., **2008**, 130 (33), 11088-11096 • DOI: 10.1021/ja8027313 • Publication Date (Web): 29 July 2008

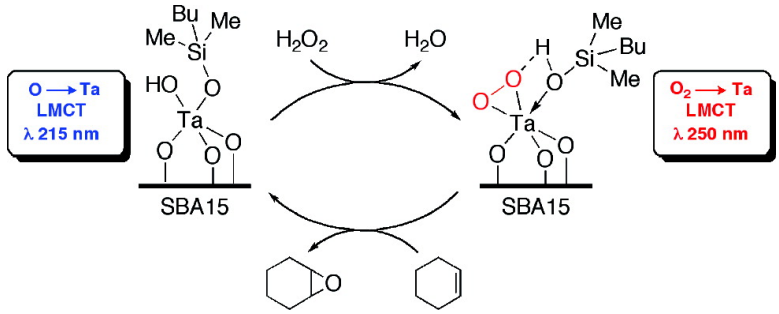

More About This Article

Additional resources and features associated with this article are available within the HTML version:

- Supporting Information
- Access to high resolution figures
- Links to articles and content related to this article
- Copyright permission to reproduce figures and/or text from this article

View the Full Text HTML

J|A|C|S
ARTICLES

Published on Web 07/29/2008

Kinetics and Mechanism of Olefin Epoxidation with Aqueous H_2O_2 and a Highly Selective Surface-Modified TaSBA15 Heterogeneous Catalyst

Daniel A. Ruddy and T. Don Tilley*

Department of Chemistry, University of California, Berkeley, California 94720, and Chemical Sciences Division, Lawrence Berkeley National Laboratory, 1 Cyclotron Road, Berkeley, California 94720

Received April 14, 2008; E-mail: tdtilley@berkeley.edu

Abstract: The reaction kinetics of cyclohexene epoxidation using aqueous H_2O_2 oxidant and the highly selective epoxidation catalyst **Bu_{cap}TaSBA15** were studied. The reaction was determined to be first-order in Ta(V) surface coverage. The reaction rate exhibited saturation with respect to increasing concentrations of cyclohexene and H_2O_2. An Eley−Rideal mechanism and rate equation may be used to describe the epoxidation kinetics, which are similar to those for Ti(IV)SiO_2-catalyzed epoxidations. The observed kinetics may also be modeled by a double-displacement mechanism typically associated with saturation enzyme catalysts. In addition, ^{1}H NMR spectroscopy was employed to investigate H_2O_2 decomposition by **Bu_{cap}TaSBA15** and the unmodified **TaSBA15** catalysts. Little decomposition occurred over the surface-modified material, but the unmodified material catalyzed a 30% conversion of H_2O_2 after 6 h. UV−visible absorbance and diffuse reflectance UV−visible (DRUV−vis) spectroscopy were used to investigate the structure of the Ta centers on the **TaSBA15** catalysts. DRUV−vis spectroscopy was also used to identify a Ta(V)-based epoxidation intermediate, proposed to be a Ta(V)(η^2-O_2) species, which forms upon reaction of the **TaSBA15** and **Bu_{cap}TaSBA15** materials with H_2O_2.

Introduction

The direct functionalization of inexpensive and readily available alkanes and alkenes to more synthetically useful oxygenated compounds remains a major challenge in catalysis research. In this context, heterogeneous, selective oxidation catalysts have attracted considerable attention for the development of low-energy, cost-effective transformations.[1−4] Selective alkene epoxidation catalysts are of particular interest, since epoxides are important synthetic intermediates for fine chemical production, and high-tonnage products such as propylene oxide are used in polyether polymer synthesis. Further advances in this field should be facilitated by the establishment of important structure−activity relationships and synthesis of new, high-performance catalysts with well-defined structures.[5,6] A well-established technique for the introduction of well-defined, site-isolated metal centers is based on the thermolytic molecular precursor (TMP) method.[7,8] In this approach, oxygen-rich metal precursor complexes are grafted onto a metal oxide support via a protonolysis reaction, and low-temperature (<200 °C) calcination is used to remove the hydrocarbon components of the precursor. This methodology has been successfully applied to the preparation of numerous site-isolated catalytic materials that demonstrate improved activity and/or selectivity in hydrocarbon oxidations.[9−13]

For surface-bound active sites, the chemical properties of the surface should play an important role in determining catalyst activity and selectivity. For example, surface properties may influence the rate of substrate adsorption or product desorption, and surface functionalities (e.g., −OH, $-NH_2$) may act to stabilize reactive catalytic centers or intermediates through secondary interactions (e.g., H-bonding).[14] These concepts are well established in the operation of enzymes, where the protein environment acts to promote substrate binding and to stabilize reactive centers.[15−17] The poor performance of Ti(IV) sites supported on mesoporous silicas in the epoxidation of alkenes

(1) Sheldon, R. A. *J. Mol. Catal.* **1980**, *7*, 107.
(2) Corma, A. *Chem. Rev.* **1997**, *97*, 2373.
(3) Lucke, B.; Narayana, K. V.; Martin, A.; Jahnisch, K. *Adv. Synth. Catal.* **2004**, *346*, 1407.
(4) Mallat, T.; Baiker, A. *Chem. Rev.* **2004**, *104*, 3037.
(5) Tilley, T. D. *J. Mol. Catal. A* **2002**, *182*, 17.
(6) Thomas, J. M.; Raja, R.; Lewis, D. W. *Angew. Chem., Int. Ed.* **2005**, *44*, 6456.
(7) Fujdala, K. L.; Tilley, T. D. *J. Catal.* **2003**, *216*, 265.
(8) Fujdala, K. L.; Brutchey, R. L.; Tilley, T. D. Tailored Oxide Materials Via Thermolytic Molecular Precursor (TMP) Methods. In *Topics in Organometallic Chemistry*; Coperet, C., Chaudret, B., Eds.; Springer-Verlag: New York, 2005; Vol. 16, pp 69−116.
(9) Jarupatrakorn, J.; Tilley, J. D. *J. Am. Chem. Soc.* **2002**, *124*, 8380.
(10) Nozaki, C.; Lugmair, C. G.; Bell, A. T.; Tilley, T. D. *J. Am. Chem. Soc.* **2002**, *124*, 13194.
(11) Brutchey, R. L.; Drake, I. J.; Bell, A. T.; Tilley, T. D. *Chem. Commun.* **2005**, 3736.
(12) Ruddy, D. A.; Ohler, N. L.; Bell, A. T.; Tilley, T. D. *J. Catal.* **2006**, *238*, 277.
(13) Holland, A. W.; Li, G. T.; Shahin, A. M.; Long, G. J.; Bell, A. T.; Tilley, T. D. *J. Catal.* **2005**, *235*, 150.
(14) Anwander, R. *Chem. Mater.* **2001**, *13*, 4419.
(15) Toone, E. J.; Simon, E. S.; Bednarski, M. D.; Whitesides, G. M. *Tetrahedron* **1989**, *45*, 5365.
(16) Merkley, N.; Shaw, G. S. *J. Biomol. NMR* **2003**, *26*, 147.
(17) Lassila, J. K.; Keeffe, J. R.; Kast, P.; Mayo, S. L. *Biochemistry* **2007**, *46*, 6883.

10.1021/ja8027313 CCC: $40.75

with aqueous hydrogen peroxide has been attributed to the chemical properties of the support surface.[18−20] The catalyst surface is hydrophilic, and the Ti(IV) site is presumably deactivated by the competitive binding of water, which hinders formation of the key titanium−hydroperoxide intermediate.[1] There is considerable interest in this problem, since aqueous hydrogen peroxide is a desirable oxidant that yields an environmentally benign byproduct (H_2O).

Several investigations over the past decade have focused on the development of catalysts that efficiently utilize hydrogen peroxide, via chemical modifications of the catalyst surface.[20−26] We have recently reported significant improvements in epoxidation activity and selectivity with **TiSBA15** and **TaSBA15** catalysts that are silylated using (*N*,*N*-dimethylamino)trialkylsilane reagents (up to 58% epoxide selectivity for Ti and >95% epoxide selectivity for Ta).[27−29] It was demonstrated that high epoxidation selectivity in these TMP-derived systems is associated with the presence of a direct $R_3Si-O-Ti$ or $R_3Si-O-Ta$ linkage at the active site; it was also shown that the presence of a hydrophobic surface alone is not sufficient to observe increased selectivity. In contrast to the **R_{cap}TiSBA15** catalyst (R = Me, Bu, or Oc), for which a key TiOOH intermediate has been identified, mechanistic considerations for the **R_{cap}TaSBA15** catalysts were proposed without structural identification of the oxidative intermediate. However, the proposed Ta(V)-(η^2-O_2) intermediate is structurally similar to numerous Mo(VI)-(η^2-O_2) and W(VI)(η^2-O_2) complexes that have demonstrated high activity and/or selectivity for the epoxidation of alkenes.[30−34]

Detailed mechanistic information, as provided by kinetic studies, is essential for establishment of a complete understanding of the factors that control catalytic efficiency, and for development of improved catalysts. For Ti(IV)SiO_2 catalysts, there have been a few kinetic and mechanistic studies, involving epoxidations of propene, allyl chloride, and cyclooctene with H_2O_2,[35−37] and cyclohexene epoxidation with *tert*-butyl hydroperoxide (TBHP).[38] In addition, the kinetics of alkene epoxidation with H_2O_2 and organic oxidants catalyzed by molecular Mo(VI) and W(VI) complexes have also yielded important information about catalytic mechanisms.[30,39−42]

This report describes a kinetic and mechanistic investigation of cyclohexene epoxidation with aqueous H_2O_2, as catalyzed by **Bu_{cap}TaSBA15(*x*)** materials (*x* = wt % Ta). The saturation kinetics observed for these reactions are interpreted in terms of an Eley−Rideal mechanism involving H_2O_2 activation followed by oxygen transfer to olefin at the Ta(V) center. In addition, spectroscopic information suggests the intermediacy of a Ta(V)(η^2-O_2) oxidative intermediate.

Table 1. Ta Content and Nitrogen Physisorption Data for **Bu_{cap}TaSBA15** Materials

material	Ta content (μmol g^{-1})	Ta coverage[a] (Ta nm^{-2})	S_{BET} (m^2 g^{-1})	r_{pore} (nm)
SBA15			680	3.3
Bu_{cap}TaSBA15(0.76)	41.8	0.0370	330	2.8
Bu_{cap}TaSBA15(1.14)	63.0	0.0558	305	2.8
Bu_{cap}TaSBA15(1.35)	74.6	0.0660	300	2.8
Bu_{cap}TaSBA15(1.68)	92.8	0.0822	300	2.8

[a] Determined using S_{BET} of SBA15, 680 m^2 g^{-1}.

Results

Materials Synthesis and Characterization. The mesoporous silica SBA15 was prepared according to a literature procedure.[43] The surface grafting chemistry of $Ta(O^iPr)_2[OSi(O^tBu)_3]_3$ (**1**) to yield **TaSBA15(*x*)**, and subsequent surface modification chemistry with Me_2N-$SiMe_2Bu$, was recently communicated.[28,44] The maximum wt % Ta attainable using **1** (prior to surface modification) is ca. 1.91 wt % Ta. Calcination of **TaSBA15(*x*)** at 200 °C under air, followed by surface modification, yields **Bu_{cap}TaSBA15(*x*)**, where *x* represents the Ta wt % as determined by inductively coupled plasma (ICP) methods.

For kinetic studies, **Bu_{cap}TaSBA15(*x*)** materials were prepared with *x* values ranging from 0.76 to 1.68 wt %. The surface area and pore structure of the materials were evaluated using nitrogen porosimetry. The N_2 adsorption−desorption data of all samples are consistent with type IV isotherms, indicative of mesoporous SBA15-like materials with narrow pore size distributions, as determined from the adsorption isotherm.[43] The Ta content, BET surface area, and pore radius data for the materials are presented in Table 1. Furthermore, these materials exhibit hydrophobic surfaces with 1.2 surface silyl groups per squre nanometer, as determined by thermogravimetric analysis (TGA) and carbon elemental analysis. These values are similar to previously reported materials prepared from **1** in the same manner.[28]

The local structure of the supported Ta(V) centers was investigated using diffuse reflectance UV−visible (DRUV−vis) spectroscopy, although it should be noted that this technique alone cannot provide an accurate description of the coordination environment for such Ta(V) centers. One advantage of the TMP method is that the molecular precursor can be used as a

(18) Corma, A.; Esteve, P.; Martinez, A. *J. Catal.* **1996**, *161*, 11.
(19) Blasco, T.; Corma, A.; Navarro, M. T.; Pariente, J. P. *J. Catal.* **1995**, *156*, 65.
(20) Tatsumi, T.; Koyano, K. A.; Igarashi, N. *Chem. Commun.* **1998**, 325.
(21) Bu, J.; Rhee, H. K. *Catal. Lett.* **2000**, *66*, 245.
(22) Bu, J.; Rhee, H. K. *Catal. Lett.* **2000**, *65*, 141.
(23) Deng, Y.; Maier, M. F. *J. Catal.* **2001**, *199*, 115.
(24) Muller, C. A.; Deck, R.; Mallat, T.; Baiker, A. *Top. Catal.* **2000**, *11*, 369.
(25) D'Amore, M. B.; Schwarz, S. *Chem. Commun.* **1999**, 121.
(26) Corma, A.; Domine, M.; Gaona, J. A.; Jorda, J. L.; Navarro, M. T.; Rey, F.; Perez-Pariente, J.; Tsuji, J.; Mcculloch, B.; Nemeth, L. T. *Chem. Commun.* **1998**, 2211.
(27) Brutchey, R. L.; Ruddy, D. A.; Andersen, L. K.; Tilley, T. D. *Langmuir* **2005**, *21*, 9576.
(28) Ruddy, D. A.; Tilley, T. D. *Chem. Commun.* **2007**, 3350.
(29) Ruddy, D. A.; Brutchey, R. L.; Tilley, T. D. *Top. Catal.* **2008**, *48*, 99.
(30) Kamata, K.; Kuzuya, S.; Uehara, K.; Yamaguch, S.; Mizuno, N. *Inorg. Chem.* **2007**, *46*, 3768.
(31) Jimtaisong, A.; Luck, R. L. *Inorg. Chem.* **2006**, *45*, 10391.
(32) Bregeault, J.-M. *Dalton Trans.* **2003**, 3289.
(33) Aubry, C.; Chottard, G.; Platzer, N.; Bregeault, J. M.; Thouvenot, R.; Chauveau, F.; Huet, C.; Ledon, H. *Inorg. Chem.* **1991**, *30*, 4409.
(34) Piquemal, J.-Y.; Halut, S.; Bregeault, J.-M. *Angew. Chem., Int. Ed.* **1998**, *37*, 1146.
(35) Liang, X. H.; Mi, Z. T.; Wu, Y. L.; Wang, L.; Xing, E. H. *React. Kinet. Catal. Lett.* **2003**, *80*, 207.
(36) Gao, H. X.; Lu, G. X.; Sue, J. H.; Li, S. B. *Appl. Catal., A* **1996**, *138*, 27.
(37) Yamase, T.; Ishikawa, E.; Asai, Y.; Kanai, S. *J. Mol. Catal. A* **1996**, *114*, 237.
(38) Notestein, J. M.; Iglesia, E.; Katz, A. *J. Am. Chem. Soc.* **2004**, *126*, 16478.
(39) Amato, G.; Arcoria, A.; Ballistreri, F. P.; Tomaselli, G. A. *J. Mol. Catal.* **1986**, *37*, 165.
(40) Wang, X. Y.; Shi, H. C.; Xu, S. Y. *J. Mol. Catal. A* **2003**, *206*, 213.
(41) Mitchell, J. M.; Finney, N. S. *J. Am. Chem. Soc.* **2001**, *123*, 862.
(42) Arcoria, A.; Ballistreri, F. P.; Tomaselli, G. A.; Difuria, F.; Modena, G. *J. Mol. Catal.* **1983**, *18*, 177.
(43) Zhao, D. Y.; Huo, Q. S.; Feng, J. L.; Chmelka, B. F.; Stucky, G. D. *J. Am. Chem. Soc.* **1998**, *120*, 6024.
(44) Brutchey, R. L.; Lugmair, C. G.; Schebaum, L. O.; Tilley, T. D. *J. Catal.* **2005**, *229*, 72.

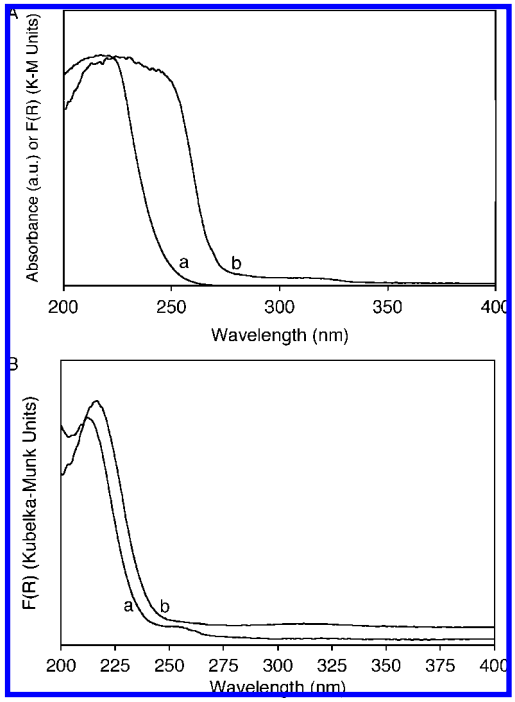

Figure 1. (A) UV−vis and DRUV−vis spectra for (a) **1** in hexanes solution and (b) **1** in the solid state. (B) DRUV−vis spectra for (a) **TaSBA15(1.91)** and (b) **Bu_{cap}TaSBA15(1.68)**.

spectroscopic model for the active site prepared after grafting. Precursor **1** was demonstrated to exist as a penta-coordinate monomer in solution, but it crystallizes with a distorted octahedral coordination environment for tantalum due to a dative interaction from a pendant *tert*-butoxy group.[44] The UV−visible absorbance spectrum of **1** in hexanes exhibits a high-energy O→Ta ligand-to-metal charge-transfer (LMCT) band centered at 215 nm, with little absorbance past 250 nm (Figure 1A, trace (a)). The solid-state DRUV−vis spectrum of **1** exhibits a broader absorption centered at 230 nm and extending to 270 nm, consistent with an increased tantalum coordination number of six (Figure 1A, trace (b)). The DRUV−vis spectra of the TMP-derived materials **TaSBA15(1.91)** (trace (a)) and **Bu_{cap}TaSBA15(1.68)** (trace (b)) are included in Figure 1B. The absorbance spectra for these materials are similar to the solution-state spectrum of **1** and exhibit a narrow LMCT band centered at 215 nm. It is worth noting, however, that pure SBA15 functionalized with a Me_3SiO cap (Me_{cap}SBA15) has a UV absorbance at 215−220 nm. Thus, the LMCT for the **Bu_{cap}TaSBA15(1.68)** material coincides with background absorbance of the surface-modified support.

H_2O_2 Decomposition Studies. The **Bu_{cap}TaSBA15(*x*)** materials were recently reported as active epoxidation catalysts over 6 h of reaction time, with high selectivity for epoxide formation versus allylic oxidation (≥95%).[28] It is also of interest to determine the efficiency of these reactions with respect to hydrogen peroxide usage. This is especially pertinent because hydrogen peroxide decomposes to form oxygen and water at elevated temperatures, and in the presence of many transition metals (e.g., V, Ti, Mn, Fe, Cu).[45] Thus, it is conceivable that the high epoxide selectivity exhibited by this catalyst could be accompanied by significant hydrogen peroxide decomposition at the Ta(V) centers, resulting in low product yields.

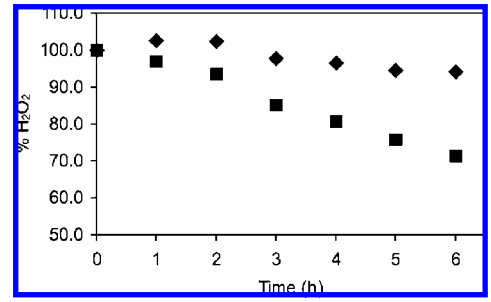

Figure 2. H_2O_2 decomposition by **TaSBA15(1.91)** (■) and **Bu_{cap}TaSBA15(1.68)** (◆) as monitored by ^{1}H NMR spectroscopy.

A recent report outlined a general method to monitor low hydrogen peroxide concentrations in a methanol/acetonitrile solution via ^{1}H NMR spectroscopy.[46] In 0.8−0.9 M solutions of H_2O_2 in acetonitrile-d_3, well-resolved resonances are observed for H_2O (δ 3.05) and H_2O_2 (δ 9.36 versus an internal standard of C_6H_6). In control experiments with no catalyst, blank SBA15, or Me_{cap}SBA15 (no Ta), the concentration of H_2O_2 remained within 95% of the initial concentration (by comparison to a C_6H_6 internal standard) throughout 6 h of heating at 65 °C. When **Bu_{cap}TaSBA15(1.68)** was added to a solution of H_2O_2 in acetonitrile-d_3 (1400 equiv of H_2O_2 vs Ta), the concentration of H_2O_2 again remained within 95% of the initial concentration for 6 h (Figure 2). However, when the unmodified **TaSBA15(1.91)** material was added to a solution of H_2O_2 (1400 equiv of H_2O_2 vs Ta), a nearly linear decrease in H_2O_2 concentration by 30% was observed over the course of 6 h at 65 °C (Figure 2). This analysis suggests that there is little hydrogen peroxide decomposition over the surface-modified catalyst. Moreover, these results confirm that the epoxide selectivity that was initially reported with respect to olefin converstion is equally high with respect to H_2O_2 (≥95%). On the other hand, these results indicate that the unmodified **TaSBA15(1.91)** catalyst slowly decomposes hydrogen peroxide under the catalytic conditions. Since decomposition is not observed in the absence of catalyst or over pure SBA15, the unmodified Ta(V) site is clearly responsible for this decomposition.

Identification of Catalytically Relevant Intermediates. To investigate the formation of a Ta-based oxidative intermediate with the **TaSBA15(*x*)** catalysts, 1 mL of a 1:1 solution of 30% H_2O_2 in acetonitrile was added to a 30 mg sample of unmodified **TaSBA15(1.91)** material, and the reaction was heated at 65 °C for 1 h. After cooling, the volatile reagents were removed *in vacuo* for 16 h. This yielded the peroxide-activated material, **$TaSBA15_{H2O2}$**. As depicted in Figure 3A, the DRUV−vis spectrum of this material exhibits an LMCT band at 215 nm with a broad shoulder at ca. 250 nm. This shoulder was not observed upon treatment of Ta-free SBA15 with H_2O_2, nor was it observed upon treatment of **TaSBA15(1.91)** with a water/acetonitrile solution. Thus, the shoulder is associated with both Ta(V) and H_2O_2 being present in the sample. Upon exposure of the **Bu_{cap}TaSBA15(1.68)** material to the peroxide solution followed by evacuation, a similar broad shoulder appeared in the DRUV−vis spectrum (Figure 3B). The new band, associated with the peroxide-activated material **$Bu_{cap}TaSBA15_{H2O2}$**, is also centered at ca. 250 nm. For both materials, this spectral feature was still observed after exposure to air for 2 h. However, introduction of a 1:1 solution of cyclohexene and acetonitrile,

(45) Salem, I. A.; El-Maazawi, M.; Zaki, A. B. *Int. J. Chem. Kinet* **2000**, *32*, 643.

(46) Stephenson, N. A.; Bell, A. T. *Anal. Bioanal. Chem.* **2005**, *381*, 1289.

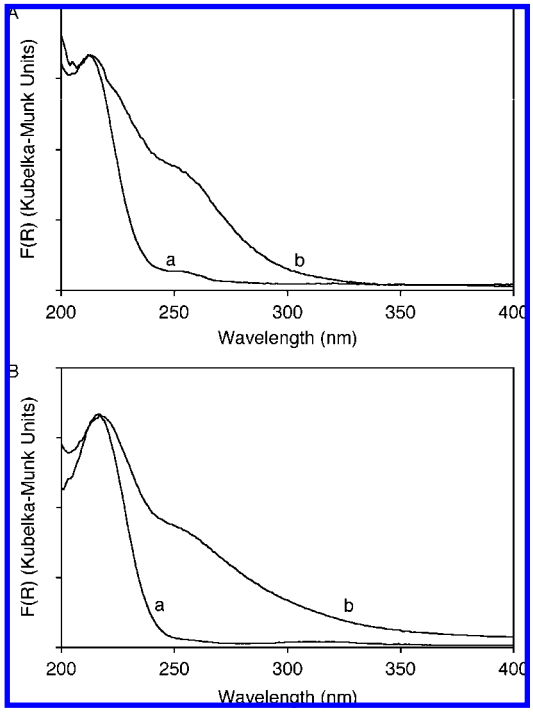

Figure 3. (A) DRUV−vis spectra of (a) **TaSBA15(1.91)** and (b) **TaSBA15$_{H2O2}$**. (B) DRUV−vis spectra of (a) **Bu$_{cap}$TaSBA15(1.68)** and (b) **Bu$_{cap}$TaSBA15$_{H2O2}$**.

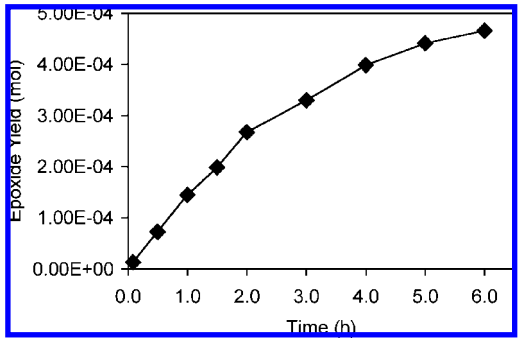

Figure 4. Kinetic plot of cyclohexene epoxidation with aqueous hydrogen peroxide in acetonitrile at 65 °C catalyzed by **Bu$_{cap}$TaSBA15(1.68)**.

followed by heating at 65 °C for 30 min, rapidly degrades this new band. In addition, the sole product of this reaction was identified as cyclohexene oxide via gas chromatographic (GC) analysis of the solution. In the case of **TaSBA15$_{H2O2}$**, the epoxide was observed in 90% yield based on the Ta(V) content (0.9 turnover). For **Bu$_{cap}$TaSBA15$_{H2O2}$**, 95% yield was observed after 30 min at 65 °C (0.95 turnover). This is strong evidence that the Ta species associated with the LMCT band near 250 nm is the active oxidant.

Epoxidation Kinetics. As previously reported, the **Bu$_{cap}$TaSBA15(x)** materials are active and selective (>95%) catalysts for the epoxidation of cyclohexene in acetonitrile with aqueous H_2O_2 over a reaction time of 6 h with no observed leaching (<5 ppm).[28] Figure 4 depicts the epoxide yield versus time, and it is clear that the epoxidation rate (d[epoxide]/dt) decreases after 2 h. Similar to Ti(IV)SiO_2 catalysts, this rate inhibition is likely due to polar species in solution (e.g., water, epoxide), which competitively bind to the Ta(V) center and decrease the catalytic turnover rate.[1] However, epoxide formation over the first hour exhibits a linear concentration increase, and therefore,

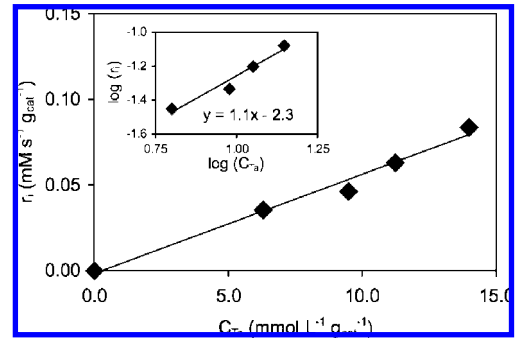

Figure 5. Plot of initial epoxidation rate versus Ta(V) surface coverage. The inset plots log(rate) versus log(Ta(V) concentration). Solid lines represent linear regressions of the data.

the kinetics during this early stage of the reaction can be easily investigated using the method of initial rates.

Initial rates of cyclohexene oxide formation were measured to determine the reaction order with respect to Ta(V) content (C_{Ta}) for the **Bu$_{cap}$TaSBA15(x)** catalysts. Measurements of epoxide formation in a batch reactor were monitored via GC analysis of aliquots (0.10 mL) taken every 15 min over the course of 1 h of reaction time. The reaction order in Ta(V) was determined by measuring the epoxide formation rates under pseudo-first-order conditions with excess cyclohexene (300−670 equiv vs Ta) and excess hydrogen peroxide (180−410 equiv vs Ta). The initial rates of epoxide formation (r_i, mM epoxide s^{-1} g_{cat}^{-1}), standardized to the mass of catalyst, vary linearly with respect to Ta(V) content over the low range of Ta(V) loadings (maximum 92.8 μmol g_{cat}^{-1}) that are synthetically accessible in this system (Figure 5). This indicates a first-order dependence of the epoxidation rate on Ta(V) content over this range, and the pseudo-first-order rate constant, k_{obs}, was determined to be 5.8(4) × 10^{-3} s^{-1} from the slope of the linear regression. A plot of log r_i versus log C_{Ta} produced a straight line with a slope of 1.1(1), verifying the first-order rate dependence on Ta(V) content (Figure 5, inset). Furthermore, a plot of the turnover number (TON, mol epoxide (mol Ta)$^{-1}$) taken at 1 h of reaction time supports single-site behavior of the Ta(V) centers, as exhibited by a constant TON value of ca. 20 (Figure S1, Supporting Information).

Initial rates of cyclohexene oxide formation (r_i, μM epoxide s^{-1} g_{cat}^{-1}) were measured to investigate the reaction order in hydrogen peroxide and cyclohexene. Measurements of the kinetics of epoxide formation were monitored via GC as described above. The reaction order in one substrate was examined by measuring the epoxide formation rates under pseudo-first-order conditions with respect to the other substrate. A **Bu$_{cap}$TaSBA15(1.22)** catalyst was employed. As depicted in Figure 6A, the initial rate of epoxide formation exhibits a saturation profile with respect to increasing initial H_2O_2 concentration ($[H_2O_2]_i$). A linear double-reciprocal plot of $1/r_i$ versus $1/[H_2O_2]_i$ confirms the saturation kinetics behavior (Figure 6A, inset). A similar saturation profile was observed when the initial epoxidation rate was measured while varying the initial concentration of cyclohexene (Figure 6B). A linear double-reciprocal plot of $1/r_i$ versus $1/[\text{cyclohexene}]_i$ was also observed (Figure 6B, inset). In both cases, the linear fit is in excellent agreement with the experimental data ($R^2 > 0.98$).

Discussion

Structural Assignment of Supported Ta(V) Centers. The initially proposed structure of the silica-supported Ta(V) center

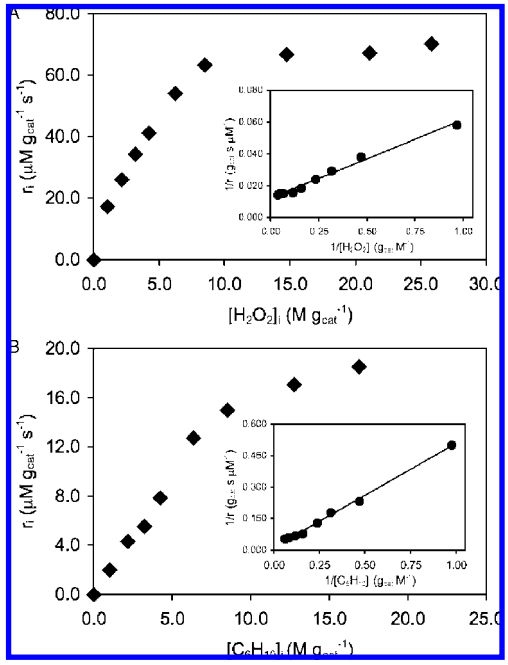

Figure 6. (A) Plot of initial epoxidation rate versus initial H_2O_2 concentration, with the double-reciprocal plot in the inset. (B) Plot of initial epoxidation rate versus initial cyclohexene concentration, with the double-reciprocal plot in the inset. The linear regressions in the double-reciprocal plots have values of $R^2 > 0.98$.

included a direct Ta−O−$SiMe_2Bu$ linkage, which was identified via solid-state magic-angle-spinning (MAS) ^{29}Si NMR spectroscopy.[28] The exact structure of the surface-bound Ta(V) species is difficult to determine, due in part to the lack of previous spectroscopic assignments of similar low wt % Ta(V) materials. UV−visible absorbance spectroscopy and the solid-state analogue, DRUV−vis spectroscopy, can be effective techniques to elucidate the local structure of supported metal oxides because the energy of the LMCT band is dependent on the metal coordination environment. In general, a red-shift in the LMCT band occurs upon increasing coordination number of the metal center and/or agglomeration of metal centers via bridging oxygen ligands.

Few previous investigations have dealt with low wt % Ta materials subjected to low-temperature calcinations similar to these **TaSBA15(*x*)** materials. DRUV−vis spectroscopic investigations of higher wt % Ta materials subjected to high-temperature calcination (500 °C) include assignments of numerous surface species: crystalline Ta_2O_5 at 265−270 nm, noncrystalline tantala at 260 nm, and isolated terminal tantalum−oxo structures at 220−235 nm.[47,48] An EXAFS evaluation of high wt % tantala−silica materials assigned the supported Ta(V) structure as a tetrahedral TaO_4 with one terminal tantalum−oxo (Ta═O).[49,50] However, these data provide a poor basis for comparison to the **TaSBA15(*x*)** and **Bu_{cap}TaSBA15(*x*)** materials prepared under much milder conditions.

The DRUV−vis spectra for the **TaSBA15(*x*)** and **Bu_{cap}TaSBA15(*x*)** materials exhibit a high-energy LMCT centered at 215 nm, which is similar to that observed for pentacoordinate **1** in hexanes and clearly differs from the spectrum of **1** with octahedral coordination in the solid state. There is no spectroscopic evidence for the existence of crystalline or noncrystalline Ta_2O_5 on the materials subjected to this mild preparation procedure. In addition, no crystallites were observed via transmission electron microscopy imaging, and powder X-ray diffraction (PXRD) patterns are characteristic of unmodified SBA15: they exhibit no diffraction peaks in the range of 2θ values from 5° to 70°. Terminal Ta═O species exhibit a characteristic stretch (ν Ta═O) in the infrared spectrum between 850 and 1000 cm^{-1}.[47,48] No such peak was observed upon transmission or diffuse reflectance FT-IR spectroscopic analysis of the materials. These spectroscopic data support the initial structural assignment of isolated tantalum centers, similar to that of **1** in solution.

Evidence for a Ta(η^2-O_2) Intermediate. In contrast to the volume of literature regarding Ti(IV)SiO_2 materials as epoxidation catalysts, Ta(V)SiO_2 materials have been much less studied. In particular, there is little evidence for related Ta(V)-based oxidation intermediates.[51−53] Studies utilizing *in situ* spectroscopic techniques have identified a titanium−hydroperoxy (TiOOH) species as the active oxidant in titania−silica-catalyzed olefin epoxidation reactions.[27,54] For molecular Mo(VI)- and W(VI)-catalyzed epoxidations, a metal−η^2-peroxo (M(η^2-O_2)) has been identified as the active oxidant.[30−33,55,56] A recent report attributes thioether oxidation over tantala−silica mixed oxides to the presence of a tantalum−η^2-peroxo intermediate; however, allylic alcohol epoxidation over $TaSiO_2$ has been associated with a tantalum−η^2-*tert*-butylperoxo.[51,53] Spectroscopic identification of the active species was not reported in either case.

The LMCT band at 250 nm in the DRUV−vis spectra of **$TaSBA15_{H2O2}$** and **$Bu_{cap}TaSBA15_{H2O2}$**, associated with reaction of the Ta(V) center with a H_2O_2 solution, is red-shifted from the parent O→Ta LMCT band at 215 nm for the supported Ta(V) center. This red-shift in the DRUV−vis spectrum is similar to that observed with Ti(IV)SiO_2 materials upon reaction with H_2O_2, where a band at 350−400 nm is observed in addition to the parent LMCT band at 250 nm.[27] In addition, the LMCT band at 250 nm for **$TaSBA15_{H2O2}$** is similar to the metal−peroxo LMCT bands for molecular Mo(VI)(η^2-O_2) species (280−310 nm) and nearly identical to that observed for molecular W(VI)(η^2-O_2) (250−270 nm) complexes.[30,33,57] Therefore, the observance of this band at 250 nm suggests the formation of a tantalum−peroxo species.

Similar to Mo(VI) and W(VI), numerous stable Ta(V)−peroxo complexes have been reported and characterized, and each one features η^2 coordination of the peroxo ligand.[58] Little attention has been given to the UV−vis absorption spectra of the Ta(V)(η^2-O_2) complexes, so $K_3Ta(O_2)_4 \cdot {}^1/_2H_2O$ (**2**) was prepared

(47) Lee, E. L.; Wachs, I. E. *J. Phys. Chem. C* **2007**, *111*, 14410.
(48) Baltes, M.; Kytokivi, A.; Weckhuysen, B. M.; Schoonheydt, R. A.; Van Der Voort, P.; Vansant, E. F. *J. Phys. Chem. B* **2001**, *105*, 6211.
(49) Ushikubo, T.; Wada, K. *Appl. Catal., A* **1995**, *124*, 19.
(50) Tanaka, T.; Nojima, H.; Yamamoto, T.; Takenaka, S.; Funabiki, T.; Yoshida, S. *Phys. Chem. Chem. Phys.* **1999**, *1*, 5235.
(51) Meunier, D.; De Mallmann, A.; Basset, J. M. *Top. Catal.* **2003**, *23*, 183.
(52) Meunier, D.; Piechaczyk, A.; De Mallmann, A.; Basset, J. M. *Angew. Chem., Int. Ed.* **1999**, *38*, 3540.
(53) Cimpeanu, V.; Parvulescu, V.; Parvulescu, V. I.; Capron, M.; Grange, P.; Thompson, J. M.; Hardacre, C. *J. Catal.* **2005**, *235*, 184.
(54) Lin, W. Y.; Frei, H. *J. Am. Chem. Soc.* **2002**, *124*, 9292.
(55) Arcoria, A.; Ballistreri, F. P.; Tomaselli, G. A.; Di Furia, F.; Modena, G. *J. Org. Chem.* **1986**, *51*, 2374.
(56) Celestin Bakala, P.; Briot, E.; Salles, L.; Bregeault, J.-M. *Appl. Catal., A* **2006**, *300*, 91.
(57) Djordjevic, C.; Puryear, B. C.; Vuletic, N.; Abelt, C. J.; Sheffield, S. J. *Inorg. Chem.* **1988**, *27*, 2926.
(58) Bayot, D.; Devillers, M. *Coord. Chem. Rev.* **2006**, *250*, 2610.

as a reference compound.[59] This complex represents a stable example of a Ta(V)(η^2-O_2) complex without additional ligands that could interfere with the Ta−O_2 LMCT band. The DRUV−vis spectrum of **2** exhibits broad LMCT bands with maxima at 225 and 250 nm (Figure S2, Supporting Information). The band at 250 nm is similar to those exhibited by the **TaSBA15$_{H2O2}$** and **Bu$_{cap}$TaSBA15$_{H2O2}$** materials, suggesting a similar species on the catalyst surface. In addition, previously described FTIR experiments support the assignment of a Ta(V)(η^2-O_2) versus a Ta(V)(OOH) intermediate.[29] Furthermore, complex **2** was found to be an active catalyst in the epoxidation of cyclohexene in acetonitrile with H_2O_2, yielding 5.6% of oxidation products with 73% epoxide selectivity after 2 h at 65 °C.[28] This result is consistent with electrophilic oxygen transfer from a Ta(V)(η^2-O_2) species and is in good agreement with the reactivity demonstrated by related W(VI)(η^2-O_2) complexes with similar spectral features.[30,33]

Mechanistic Considerations. The observed first-order rate dependence on Ta(V) concentration is consistent with the observations for similar early transition metal epoxidation catalysts. For example, the kinetics of alkene epoxidation catalyzed by various Ti(IV)SiO_2 catalysts, including TS-1, have been reported with first-order, single-site dependence on the Ti(IV) concentration.[36,38,60] Silica-supported Ti(IV) catalysts prepared via the TMP method have also exhibited single-site catalytic behavior for alkene epoxidation over a range of Ti(IV) loadings.[9,61] Furthermore, molecular Mo(VI) and W(VI) catalysts have demonstrated first-order rate dependence on catalyst concentration.[30,40−42]

For heterogeneous oxidation catalysts, it is often difficult to define elementary reaction steps and propose accurate mechanisms. This is especially true for high-temperature processes (e.g., methane partial oxidation), and for lower temperature processes where radicals play an important role (e.g., liquid-phase alkane oxidation). Many proposed mechanisms for gas-phase reactions over a heterogeneous catalyst are based on early work by Langmuir, where adsorption and desorption equilibria are incorporated into the elementary steps to describe reactions that occur between adsorbed species (Langmuir−Hinshelwood mechanism).[62] The Eley−Rideal mechanism relies on similar equilibria, but describes the direct reaction between one unadsorbed species with an adsorbed species. This mechanism has been used to describe the TS-1-catalyzed epoxidations of propene and allyl chloride with H_2O_2.[35,36] Saturation kinetics were also observed for the TS-1 catalyst, and similarly, the Eley−Rideal mechanism can be analogously employed to describe the **Bu$_{cap}$TaSBA15**-catalyzed epoxidation of cyclohexene. For such a mechanism, the elementary steps are presented in eqs 1–4, and the rate law follows the expression in eq 5.[36,63]

$$[\mathrm{Ta}] + \mathrm{H_2O_2} \overset{K_1}{\rightleftharpoons} [\mathrm{Ta{\cdot}H_2O_2}] \quad \text{(fast)} \tag{1}$$

$$[\mathrm{Ta}] + \text{alkene} \overset{K_2}{\rightleftharpoons} [\mathrm{Ta{\cdot}alkene}] \quad \text{(fast)} \tag{2}$$

$$[\mathrm{Ta{\cdot}H_2O_2}] + \text{alkene} \overset{k}{\rightleftharpoons} [\mathrm{Ta}] + \text{epoxide} + \mathrm{H_2O} \quad \text{(slow)} \tag{3}$$

$$[\mathrm{Ta}] + \text{epoxide} \overset{K_3}{\rightleftharpoons} [\mathrm{Ta{\cdot}epoxide}] \tag{4}$$

$$\frac{\mathrm{d[epoxide]}}{\mathrm{d}t} = \frac{kK_1[\mathrm{Ta}][\mathrm{H_2O_2}][\text{alkene}]}{1 + K_1[\mathrm{H_2O_2}] + K_2[\text{alkene}] + K_3[\text{epoxide}]} \tag{5}$$

There are a number of assumptions associated with this model, as previously reported.[35,36] The most notable assumptions are (i) the epoxidation takes place between adsorbed peroxide at Ta and an alkene in the free state (eq 3), (ii) the surface reaction to produce epoxide is rate-controlling with all adsorptions in equilibrium, and (iii) $K_1 \gg K_2$, that is, H_2O_2 is not in competition with alkene for active site binding. One might expect rate inhibition due to the presence of water, but this was not independently investigated. Due to the high concentration of water present under the experimental conditions employed (ca. 4 M), it is assumed that the change in water concentration is negligible at the short reaction times tested (i.e., [H_2O] can be considered constant). Epoxide-dependent rate inhibition, which can occur as epoxide concentration increases, is represented by eq 4 and with the term K_3[epoxide] in the denominator of the rate equation; similar observations were made for propene epoxidation.[35] However, at the low conversions studied here, this term is negligible, and the rate equation simplifies to that in eq 6.

$$\frac{\mathrm{d[epoxide]}}{\mathrm{d}t} = \frac{kK_1[\mathrm{Ta}][\mathrm{H_2O_2}][\text{alkene}]}{1 + K_1[\mathrm{H_2O_2}] + K_2[\text{alkene}]} \tag{6}$$

The proposed rate equation is consistent with the observed kinetics. For example, at high [H_2O_2] and high [alkene], these concentrations are essentially constant, and the observed rate equation simplifies to a first-order dependence on catalyst loading as in eq 7. Under pseudo-first-order conditions with a high [alkene]/[H_2O_2] ratio, the concentration of alkene remains constant, and the rate equation becomes indicative of saturation kinetics with respect to increasing H_2O_2 concentration, as given in eq 8. Similarly, under pseudo-first-order conditions with a high [H_2O_2]/[alkene] ratio, the rate equation becomes indicative of saturation kinetics with respect to alkene concentration, as given in eq 9.

$$\frac{\mathrm{d[epoxide]}}{\mathrm{d}t} = k_{\mathrm{obs}}[\mathrm{Ta}] \tag{7}$$

$$\frac{\mathrm{d[epoxide]}}{\mathrm{d}t} = \frac{k'_{\mathrm{obs}}[\mathrm{Ta}][\mathrm{H_2O_2}]}{K' + K_1[\mathrm{H_2O_2}]} \tag{8}$$

$$\frac{\mathrm{d[epoxide]}}{\mathrm{d}t} = \frac{k''_{\mathrm{obs}}[\mathrm{Ta}][\text{alkene}]}{K'' + K_2[\text{alkene}]} \tag{9}$$

Although this model provides an accurate stepwise mechanism and rate equation to describe the catalyst−oxidant and catalyst−substrate interactions leading to epoxidation, it does not provide the identity of precise structural intermediates for the reaction pathway. In particular, the proposed oxidative intermediate from DRUV−vis studies, Ta(V)(η^2-O_2), is represented as a simple [Ta·H_2O_2] interaction. To involve discrete molecular species in the proposed mechanism, it may prove informative to incorporate methods and models associated with homogeneous and enzyme catalysis into the analyses of heterogeneous catalysts. Models for enzyme catalysts are particularly interesting since equilibrium steps associated with enzyme mechanisms resemble those proposed in Langmuir−Hinshelwood and Eley−Rideal mechanistic analyses. For example, enzymatic processes are often characterized by kinetic profiles exhibiting saturation, and these are described by the

(59) Dengel, A. C.; Griffith, W. P. *Polyhedron* **1989**, *8*, 1371.
(60) Sheldon, R. A.; Van Doorn, J. A. *J. Catal.* **1973**, *31*, 427.
(61) Brutchey, R. L.; Mork, B. V.; Sirbuly, D. J.; Yang, P. D.; Tilley, T. D. *J. Mol. Catal. A* **2005**, *238*, 1.
(62) van Santen, R. A.; Neurock, M. *Molecular Heterogeneous Catalysis*; Wiley-VCH Verlag GmbH & Co. KGaA: Weinheim, Germany, 2006.

Scheme 1

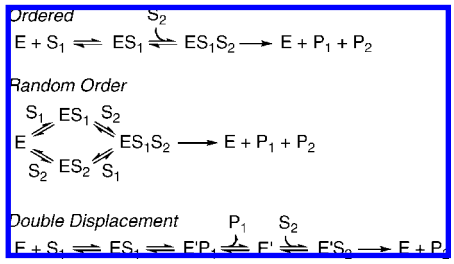

Michaelis−Menten rate equation, rate = k[cat][S]/(K_M + [S]). This expression is similar to the rate equations derived from the Eley−Rideal rate equation described above. Given the highly selective and multicomponent nature of the **Bu$_{cap}$TaSBA15(x)** catalyst, it is perhaps of interest to compare kinetic models developed for enzymes and heterogeneous catalysts.

The Michaelis−Menten equation describes the behavior of a reaction catalyzed by a single-substrate enzyme. For a two-substrate system, three mechanisms are commonly observed (Scheme 1).[64] Equilibria between the enzyme (E) and substrates (S_1, S_2) can be random or ordered, with formation of a ternary complex (ES_1S_2) followed by generation of products (P_1, P_2). In contrast, a double-displacement mechanism, with no ternary complex, can be the operative pathway. In this mechanism, the enzyme reacts with S_1 to form P_1 and an altered enzyme structure (E′). This E′ species further reacts with S_2 to form P_2 and regenerate the initial enzyme structure, E. To distinguish between a mechanism involving the formation of a ternary complex and a double-displacement mechanism, a series of double-reciprocal plots can be constructed. Measuring the initial rate for the catalyzed reaction of low concentrations of H_2O_2 (S_1) with excess concentrations of cyclohexene (S_2) results in a double-reciprocal plot for each S_2 concentration. If the linear fits for the series of plots intersect upon extrapolation to the x-axis, a ternary complex forms in the mechanism, whereas parallel linear fits are diagnostic of a double-displacement mechanism.[64]

Figure 7 displays the data of $1/r_i$ versus $1/[H_2O_2]_i$ for epoxidation catalyzed by **Bu$_{cap}$TaSBA15(1.68)** with initial H_2O_2 concentrations varying between 0.037 and 0.15 M (74−300 equiv vs Ta) and cyclohexene concentrations of 1.2, 1.5, and 1.8 M (2400, 3000, an 3600 equiv vs Ta). The plots produce parallel lines, which do not intersect upon extrapolation to the

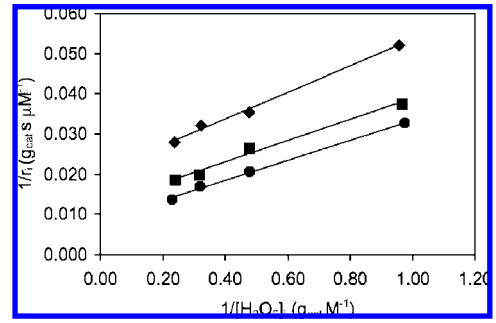

Figure 7. Double-reciprocal plots for Ta(V)-catalyzed epoxidations with initial [H_2O_2] between 0.037 and 0.15 M and [cyclohexene] of 1.2 (◆), 1.5 (■), and 1.8 (●) M.

Scheme 2

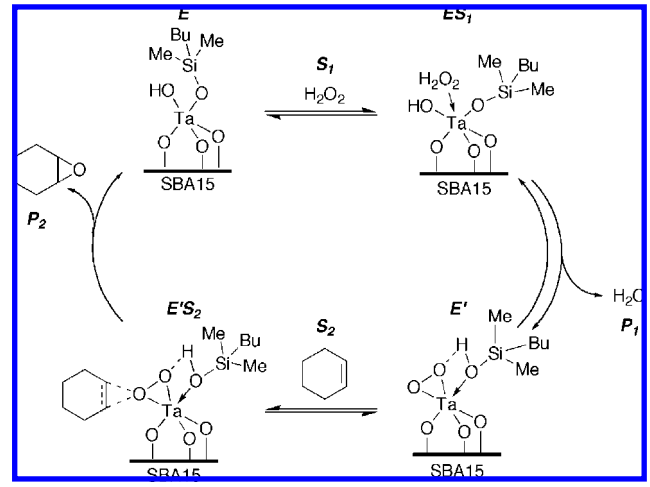

x-axis. This is indicative of a double-displacement mechanism, suggesting that the Ta(V) species reacts with one substrate, forms an intermediate, and then reacts with the other substrate to generate epoxide. This can be envisioned mechanistically as depicted in Scheme 2, with species labeled analogously to those in Scheme 1. These structures are consistent with previously proposed mechanisms of early transition metal-based epoxidations, in which an oxidative intermediate forms upon reaction of the catalytic center with the peroxide, followed by oxygen transfer to the alkene in a separate step.[1,35,36,54] This mechanism is also consistent with the formation of a Ta(V)(η^2-O_2) intermediate as described above. Hydrogen-bonding interactions with peroxo species, similar to that in the E′ structure of Scheme 2, have been calculated to be critical for Ti(IV)-based oxidations and for oxidations with H_2O_2 in fluorinated alcohol solvents.[65,66] In addition, H-bonding between protons and Mo(VI)- and W(VI)(η^2-O_2) complexes was determined to be an important factor influencing the epoxidation rate with H_2O_2 as the oxidant.[40,67] Therefore, this interaction is believed to have a marked effect on the epoxidation activity and selectivity with the **Bu$_{cap}$TaSBA15(x)** catalysts, especially since the presence of the Ta-OSiMe$_2$Bu siloxy group appears to be important for determining the observed selectivity. In addition, the Ta-bound siloxy group appears to facilitate a more efficient use of H_2O_2, in suppressing H_2O_2 disproportionation pathways. This may result from a hydrogen-bonding interaction between the two

(63) The reaction of [Ta·alkene] with H_2O_2 to form products is considered kinetically irrelevant based on the following considerations. The high-valent metal-catalyzed epoxidation of olefins with peroxide oxidant has been identified through numerous previous studies as an electrophilic oxygen-transfer reaction for many early transition-metal catalysts (Ti, V, Mo, W, Re). The proposed mechanism involves the nucleophilic attack of an olefin on a metal−peroxo species. This is true for both homogeneous and heterogeneous catalysts.[1] This is supported by the fact that electron-deficient olefins are less active (or not active) toward epoxidation. In addition, d^0 metal centers are known to activate H_2O_2 via similar pathways, but not olefins (toward reaction with H_2O_2). Therefore, nucleophilic attack of H_2O_2 onto an electron-deficient Ta(V)-bound alkene is not consistent with the well-established character of these epoxidations as electrophilic oxygen transfers. We have previously described experiments that support the similarities between the epoxidation chemistry associated with these supported Ta(V) centers and other early transition metal-catalyzed epoxidations with peroxide oxidants.[28] In addition, the proposed reaction sequence ([Ta·H_2O_2] + alkene) was established by the stepwise addition of H_2O_2 and then cyclohexene to the **TaSBA15** and **Bu$_{cap}$TaSBA15** materials, and epoxide was identified as the sole product .

(64) Cook, P. F.; Cleland, W. W. *Enzyme Kinetics and Mechanism*; Garland Science: London, 2007.

(65) Neurock, M.; Manzer, L. E. *Chem. Commun.* **1996**, 1133.

(66) Berkessel, A.; Adrio, J. A. *J. Am. Chem. Soc.* **2006**, *128*, 13412.

(67) Kamata, K.; Yamaguchi, K.; Mizuno, N. *Chem. Eur. J.* **2004**, *10*, 4728.

ligands in a Ta(η^2-O_2)(HOSiMe$_2$R) intermediate, which promotes O-atom transfer. The double-reciprocal plot analysis supports the stepwise oxygen-transfer process, which bears many similarities to the double-displacement mechanism commonly associated with enzyme catalysis.

Conclusions

Considering the interest in efficient utilization of aqueous H_2O_2 for selective oxidations, it is important to identify selective catalysts for such reactions, and to characterize the mechanisms by which they operate. The surface-modified Ta(V) catalysts described here do not decompose H_2O_2, even after 6 h at 65 °C, and demonstrate excellent epoxidation selectivity (>95%) with respect to the oxidant. This can be attributed in part to the local active-site structure, which was synthetically controlled by the TMP method to selectively yield uniform, site-isolated Ta(V) centers that were further modified with a monofunctional surface capping agent. From the kinetic analysis of cyclohexene epoxidation with the **Bu$_{cap}$TaSBA15(*x*)** catalysts, it was determined that the epoxidation is first-order in Ta(V) concentration, and saturation kinetics were observed for increasing H_2O_2 and cyclohexene concentrations. An Eley−Rideal mechanism and a double-displacement mechanism were used to model the observed kinetics. The selectivity for oxygen transfer versus allylic oxidation demonstrated by the **Bu$_{cap}$TaSBA15(*x*)** catalysts can be further credited to the nature of the oxidative intermediate, which has been identified by DRUV−vis experiments as a Ta(V)(η^2-O_2) species. It has been demonstrated that this peroxo species, formed upon reaction of **TaSBA15(*x*)** or **Bu$_{cap}$TaSBA15(*x*)** with H_2O_2, stoichiometrically oxidizes cyclohexene to yield the epoxide as the only product. Based on the high susceptibility of the Ta(V)(η^2-O_2) intermediate to undergo electrophilic oxygen transfer, surface-supported η^2-peroxo species warrant further investigation to define the breadth of their reactivity. With this in mind, these Ta(V) catalysts hold potential as potent oxidation catalysts for a broad range of substrates. Furthermore, the role of surface functionalities in promoting oxygen transfer through secondary interactions (e.g., H-bonding) is yet to be fully understood and utilized.

Experimental Procedures

General. All manipulations were conducted under a nitrogen atmosphere using standard Schlenk techniques or in a Vacuum Atmospheres drybox, unless otherwise noted. Dry, oxygen-free solvents were used throughout. Tantalum(V) chloride was purchased from Strem Chemicals, Inc. and sublimed prior to use. (*N*,*N*-Dimethylamino)butyldimethylsilane was purchased from Gelest, Inc. and used without further purification. Acetonitrile was purchased from Aldrich and distilled from P_2O_5 prior to use. Cyclohexene was purchased from Aldrich and dried over CaH_2 prior to use. Aqueous hydrogen peroxide (30%) was purchased from EM Science and used as received. The following were prepared according to literature procedures: Ta(O^{t}Pr)$_2$[OSi(O^{t}Bu)$_3$]$_3$ (**1**),[44] SBA15,[43] (^{t}BuO)$_3$SiOH,[68] $K_3Ta(O_2)_4 \cdot {}^1/_2H_2O$ (**2**),[59] **TaSBA15(*x*)**,[28] and **Bu$_{cap}$TaSBA15(*x*)**.[28]

Characterization. Benzene-d_6 was purified and dried by vacuum distillation from sodium/potassium alloy. Solution ^{1}H NMR spectra were recorded at 400 MHz using a Bruker AVB-400 spectrometer. Chemical shifts for ^{1}H NMR spectra were referenced internally to the residual solvent proton signal relative to tetramethylsilane. Nitrogen adsorption isotherms were obtained using a Quantachrome Autosorb 1, and samples were outgassed at 120 °C for at least 15 h prior to measurement. The Brunauer−Emmet−Teller (BET) method[69] was used to determine surface areas, and the Barrett−Joyner−Halenda (BJH) method[70] was used to obtain pore size distributions. Solution UV−visible absorption spectra were recorded using a Varian-Cary 300 Bio spectrophotometer. DRUV−vis spectra were obtained using a LabSphere DRA-CA-30I diffuse-reflectance attachment with the Varian-Cary 300 Bio spectrophotometer. MgO was used as the reference background material. Thermal analyses were performed on a TA Instruments SDT 2960 Integrated TGA/DSC analyzer with a heating rate of 10 °C min^{-1} under a flow of nitrogen or oxygen. Calcinations were performed using a Lindberg 1200 °C three-zone furnace with a heating rate of 10 °C min^{-1} under a flow of air, and the temperature was held constant for 4 h. Carbon and hydrogen elemental analyses were performed by the College of Chemistry microanalytical laboratory at the University of California, Berkeley. Tantalum elemental analyses were performed at Galbraith Laboratories, Inc. (Knoxville, TN) by ICP methods. PXRD experiments were performed on a Siemens D5000 X-ray diffractometer using Cu Kα radiation. GC analyses were performed with an HP 6890N system using a HP-5 phenyl methyl siloxane capillary (30.0 m × 320 μm × 0.25 μm nominal), and integration was performed relative to toluene. The mesoporous support, SBA15, was characterized by PXRD and N_2 porosimetry prior to catalyst preparation (surface area, 680 m^2 g^{-1}; pore volume, 0.81 cm^3 g^{-1}; average pore radius, 3.3 nm). The hydroxyl group concentration of the SBA15 was determined to be 1.9(1) OH nm^{-2}, via reaction of SBA15 with Mg(CH$_2$C$_6$H$_5$)$_2$·2THF and quantification of the evolved toluene by ^{1}H NMR spectroscopy.[71]

Hydrogen Peroxide Decomposition. In a J. Young NMR tube, 3.5 mg of catalyst was suspended in 0.50 mL of CD_3CN. Benzene (5.0 μL, 5.59 × 10^{-5} mol) was added as an internal standard. Hydrogen peroxide (50.0 μL, 4.89 × 10^{-5} mol) was added via syringe at room temperature. The solution was shaken and then placed in a 65 °C oil bath. A ^{1}H NMR spectrum was collected at 1-h intervals over 6 h. The concentration of hydrogen peroxide was determined via relative peak integration versus benzene.

Identification of Reactive Intermediates. Peroxide-activated **TaSBA15** and **Bu$_{cap}$TaSBA15** were prepared via addition of 1 mL of a 1:1 solution of 30% H_2O_2 and acetonitrile to 30 mg of catalyst, followed by heating at 65 °C for 30 min. The volatile components of the reaction were removed *in vacuo* at room temperature for 16 h to yield **TaSBA15$_{H2O2}$** or **Bu$_{cap}$TaSBA15$_{H2O2}$**. The colorless powder was transferred to a DRUV−vis sample holder in a drybox. Reaction of the peroxide-activated material with cyclohexene was performed via addition of 1 mL of a 1:1 solution of cyclohexene and acetonitrile (with 23 μL of toluene internal standard) to 30 mg of the **TaSBA15$_{H2O2}$** or **Bu$_{cap}$TaSBA15$_{H2O2}$** material, followed by heating at 65 °C for 30 min. A sample (0.08 mL) was removed, filtered, diluted to 0.5 mL, and analyzed by GC. The volatile components were removed *in vacuo* at room temperature for 16 h, followed by DRUV−vis analysis.

Catalysis Procedure To Determine the Reaction Order in Ta. A sample of catalyst (ca. 35 mg) with a Ta wt % value of 0.76, 1.14, 1.35, or 1.68 was added to a 50 mL three-neck round-bottom flask fitted with a reflux condenser and a septum. Acetonitrile (5.0 mL) and cyclohexene (1.0 mL, 9.9 mmol) were added via syringe through the septum under a flow of nitrogen. Toluene (23 μL) was added as an internal standard. The mixture was allowed to equilibrate at the reaction temperature of 65 °C for 10 min. Hydrogen peroxide (0.62 mL, 6.07 mmol) was added via syringe to the rapidly stirring solution. Aliquots (ca. 0.10 mL) were removed from the reaction mixture by syringe and then filtered and cooled. The filtrate was diluted with acetonitrile to 0.5 mL and analyzed

(68) Abe, Y.; Kijima, I. *Bull. Chem. Soc. Jpn.* **1969**, *42*, 1118.

(69) Brunauer, S.; Emmett, P. H.; Teller, E. *J. Am. Chem. Soc.* **1938**, *60*, 309.

(70) Barrett, E. P.; Joyner, L. G.; Halenda, P. P. *J. Am. Chem. Soc.* **1951**, *73*, 373.

(71) Fujdala, K. L.; Tilley, T. D. *J. Am. Chem. Soc.* **2001**, *123*, 10133.

by GC. Product assignments were made by comparison with the authentic samples analyzed under identical conditions.

Catalysis Procedure To Determine the Reaction Order in Cyclohexene. A sample of **Bu_{cap}TaSBA15(1.22)** catalyst (ca. 35 mg) and a toluene (23 μL) internal standard were added as before. The concentration of cyclohexene was varied between 0.040 and 0.59 M (0.025−0.40 mL), while keeping the volume of acetonitrile plus cyclohexene constant at 6.0 mL. Hydrogen peroxide (0.62 mL, 6.07 mmol) was added via syringe to the rapidly stirring solution. Aliquots (ca. 0.10 mL) were removed from the reaction mixture by syringe and then filtered and cooled. The filtrate was diluted with acetonitrile to 0.3 mL and analyzed by GC.

Catalysis Procedure To Determine the Reaction Order in Hydrogen Peroxide. A sample of **Bu_{cap}TaSBA15(1.22)**catalyst (ca. 35 mg) and a toluene (23 μL) internal standard were added as before. Acetonitrile (5.0 mL) and cyclohexene (1.0 mL, 9.9 mmol) were added via syringe through the septum under a flow of nitrogen. The hydrogen peroxide concentration was controlled via dilution of 30% H_2O_2 solution with distilled water to values of 0.037 and 0.91 M (0.025−0.62 mL), and the volume was kept constant at 0.62 mL. Aliquots (ca. 0.10 mL) were removed from the reaction mixture by syringe and then filtered and cooled. The filtrate was diluted with acetonitrile to 0.3 mL and analyzed by GC.

Acknowledgment. The authors gratefully acknowledge the support of the Director, Office of Energy Research, Office of Basic Energy Sciences, Chemical Sciences Division, of the U.S. Department of Energy under Contract DE-AC03-76SF00098. We thank A. M. Stacy at the University of California, Berkeley, for use of instrumentation (PXRD), and H. M. Frei at Lawrence Berkeley National Laboratory for helpful discussions.

Supporting Information Available: Turnover numbers for **Bu_{cap}TaSBA15(*x*)** catalysts with *x* values ranging from 0.76 to 1.68. DRUV−vis spectrum of compound **2**. This material is available free of charge via the Internet at http://pubs.acs.org.

JA8027313